A graph-based model framework for steady-state load flow problems of general multi-carrier energy systems

Markensteijn, A. S.; Romate, J. E.; Vuik, C.

DOI
10.1016/j.apenergy.2020.115286

Publication date
2020

Document Version
Final published version

Published in
Applied Energy

Citation (APA)
Markensteijn, A. S., Romate, J. E., & Vuik, C. (2020). A graph-based model framework for steady-state load flow problems of general multi-carrier energy systems. *Applied Energy*, *280*, Article 115286. https://doi.org/10.1016/j.apenergy.2020.115286

Applied Energy 280 (2020) 115286

Contents lists available at ScienceDirect

Applied Energy

journal homepage: www.elsevier.com/locate/apenergy

A graph-based model framework for steady-state load flow problems of general multi-carrier energy systems☆

A.S. Markensteijn[a,*], J.E. Romate[a,b], C. Vuik[a]

[a] Delft Institute of Applied Mathematics, Delft University of Technology, Netherlands
[b] Shell Global Solutions International B.V., Netherlands

HIGHLIGHTS

- Integrated steady-state load flow model for general multi-carrier energy system.
- Multi-carrier network description based on graph-theory.
- Coupling node allows for bidirectional flow.
- Coupling node able to represent a variety of coupling components.
- Insight into existence and uniqueness of a solution to integrated load flow problems.

ARTICLE INFO

Keywords:
Gas networks
Heat networks
Integrated energy systems
Load flow analysis
Multi-carrier energy networks
Power grids

ABSTRACT

Coupling single-carrier networks into multi-carrier energy systems (MESs) has recently become more important. Conventional load flow models for the separate single-carrier networks are not able to capture the full extend of the coupling. Recently, different models for multi-carrier energy networks have been proposed, either using the energy hub (EH) concept, or using a case specific approach. Although the EH concept can be applied to a general MES, it is unclear how the EH should be represented in the graph of the MES. On the other hand, the case specific approaches are not easily applicable to general MESs. This paper presents a graph-based framework for steady-state load flow analysis of general MESs. Furthermore, the effect of coupling on the resulting integrated system of equations is investigated. The proposed framework is validated using a small MES. This example shows that our framework is applicable to a general MES, and that it generalizes both the EH concept and the case specific approach.

1. Introduction

Multi-carrier energy systems (MESs) have recently become more important, as the need for efficient, reliable, and low carbon energy systems increases. In MESs, different energy carriers, such as electricity and heat, interact with each other, leading to one integrated system. Hence, MESs are sometimes called integrated energy systems. These energy systems have higher performance than classical single-carrier (SC) energy systems due to increased flexibility, reliability, use of renewables and distributed generation, and reduced carbon emission. An overview of MESs is given in [1].

An important tool for the design and operation of energy systems is steady-state load flow analysis, where the (different) time scales of the different systems play no role. For load flow analysis, energy systems are mathematically abstracted to a graph or network. Load flow models for single-carrier networks (SCNs) have been widely studied, but load flow models for multi-carrier networks (MCNs) have only been proposed recently. Two types of models can be distinguished. The first uses the energy hub (EH) concept, the other a case specific approach.

The energy hub (EH) concept was first introduced in [2], and models a coupling between different energy carriers by relating the input and output energy of the EH through a coupling matrix. Unidirectional flow from input to output is assumed, such that the coupling matrix is constant or a function of the input power only. Within the EH, transmission of the energy of each carrier is not taken into account. In [3,4], the EH concept is extended to allow for bidirectional flow, based

☆ This research received funding from the Netherlands Organization for Scientific Research (NWO), Alliander N.V., and Amsterdam Institute for Advanced Metropolitan Solutions (AMS).

* Corresponding author.
E-mail address: A.S.Markensteijn@tudelft.nl (A.S. Markensteijn).

https://doi.org/10.1016/j.apenergy.2020.115286
Received 8 April 2020; Received in revised form 13 May 2020; Accepted 28 May 2020

Nomenclature

Abbreviations

GHV	gross heating value.
AC	alternating current.
BC	boundary condition.
CHP	combined heat and power plant.
EH	energy hub.
GB	gas boiler.
GG	gas-fired generator.
MCN	multi-carrier network.
MES	multi-carrier energy system.
NR	the Newton-Raphson method.
SC	single-carrier.
SCN	single-carrier network.

Roman symbols

a	Parameter for a gas-fired generator, taking into account the valve-point effect.
b	Parameter for a gas-fired gener ator, taking into account the valve-point effect.
b	Susceptance, the imaginary part of y
C	Pipe constant.
C_p	Specific heat of water.
c	Parameter for a gas-fired gener ator, taking into account the valve-point effect.
D	Scaling matrix.
D	Diameter of a pipe or line.
d	Parameter for a gas-fired gener ator, taking into account the valve-point effect.
$\mathcal{E}$	Set of links or edges.
E	Energy.
e	Link or edge.
e	Error of the Newton-Raphson method.
e	Parameter for a gas-fired genera tor, taking into account the valve-point effect.
F	System of (nonlinear) load flow equations.
f	Fanning friction factor of a pipe.
$\mathcal{G}$	Graph.
g	Conductance, the real part of y.
g	Gravitational constant.
h	Head.
I	Current.
$\imath$	Imaginary unit.
J	Jacobian matrix.
L	Length of a pipe or line.
m	Water mass flow rate.
$\mathcal{N}$	Network.
P	Active power, the real part of S
p	Pressure.
	Reactive power, the imaginary part of S.
q	Gas flow rate.
r	Compressor ratio.
r	Resistance, the real part of z.
R_{air}	Specific gas constant of air.
Re	Reynolds number.
S	Complex power, given by $P + \imath Q$
S	Specific gravity.
T	Temperature.
$\mathcal{T}$	Set of terminal links.
t	Terminal link.
$\mathcal{V}$	Set of nodes or vertices.
$\lvert V\rvert$	Voltage amplitude.
V	Voltage, with angle δ and amplitude $\lvert V\rvert$.
v	Node or vertex.
x	Reactance, the imaginary part of z.
$\boldsymbol{x}$	Vector of variables.
y	Admittance, given by $g + \imath b$.
Z	Compressibility factor.
z	Impedance, given by$r + \imath x$.

Greek symbols

Δ	Difference.
δ	Voltage angle.
ε	Relative roughness of a pipe.
η	Efficiency.
λ	Heat transfer coefficient.
μ	Kinematic viscosity.
ν	Dispatch factor.
ϕ	Heat power.
ρ	Density.

Superscripts

a	Ambient.
c	Coupling.
ΔT	Temperature difference.
e	Electricity.
end	End of a link, directly next to the node.
g	Gas.
h	Heat.
I	Kirchhoff's current law.
k	Iteration of the Newton-Raphson method.
L	Link or link equation.
m	Conservation of mass (in the heat network).
min	Minimum produced.
o	Outflow; directly after a heat exchanger.
P	Conservation of energy, specifically of active power.
ψ	Thermal link equation.
	Conservation of energy, specifically of reactive power.
q	Conservation of mass (in gas network).
r	Return line.
S	Conservation of energy.
s	Supply line.
start	Beginning of a link, directly next to the node.
T	Mixing-rule.
TL	Terminal link.

Subscripts

a	Actual value.
b	Base value.
CHP	combined heat and power plant.
F	Function.
GB	gas boiler.
GG	gas-fired generator.
i	Node index.
in	Flow coming into a node, with respect to actual direction of flow
j	Node index.
k	Link index.
l	Terminal link index.
n	Index of matrix or vector.

n	At standard conditions.	p.u.	Per unit value.
out	Flow going out of a node, with respect to actual direction of flow.	x	Variable.

on graph and network theory. They provide detailed graph representations of energy flows within an EH. However, the connection of the EH to the rest of the network is not described, such that load flow analysis for the entire network is not possible. In [5], the EH concept is extended by explicitly modeling the connection between the EH and the rest of the network. All local energy generation is included in the EH. Although their extension provides a load flow model for the entire MES, they assume the output power of the EH to be a linear function of the input power. Moreover, the EH is not described as a node or link, such that the graph representation of the EH is unclear.

The second type of load flow models for MESs combines the existing equations for the SCNs and models for the coupling units into one system of equations. This allows for load flow analysis of the full MES, and for a more detailed model of the coupling units. This approach is used in [6,7] to model a combined electricity and gas network, in [8,9] to model a combined electricity and heat network, and in [10–12] to model a combined electricity, gas, and heat network. However, they do not specify how to integrate the single-carrier models using a general coupling component, making it difficult to use this approach for a general MES.

The load flow models for MES encountered so far do not state how the graphs of SCNs can be combined into one MCN. A good description of integrated networks of multiple energy carriers is very important. Some couplings between energy systems, while possible in practice, can lead to model problems. In this paper, we provide a systematic analysis of the SCNs to determine how energy systems of different carriers can be combined into one MCN.

Furthermore, the available load flow models for MES do not consider the effect of coupling on the load flow models. Usually, a coupling model introduces more unknowns than equations. Additional equations or boundary conditions (BCs) are needed for the total system to be solvable. In the models encountered so far, some or all of the energy flows to or from the couplings are assumed known as additional BCs. However, this effectively decouples the integrated load flow model of the MES into the separate single-carrier parts, such that the flexibility provided by coupling the energy systems into one MES is not fully modeled. To obtain a truly integrated model description of a MES, the additional BCs must be imposed elsewhere in the MCN. Not all combinations of load flow equations and BCs for such integrated energy systems (consisting of gas, electricity, and heat) lead to well-posed problems. For good solvability of the integrated load flow problem, the BCs used are of primary importance. In this work we give a thorough mathematical analysis of the required BCs.

Based on the systematic analysis of the SCNs and on the thorough analysis of the BCs, we propose a new graph-based model framework for steady-state load flow problems of general MESs. A comprehensive definition of a single-carrier energy system as a SCN, with corresponding load flow models for the network elements, allows for a systematic analysis of coupling SCNs into MCN. Similarities of the different carriers are exploited to define a network representation of a general energy system. We introduce a coupling node to couple the the various energy systems. Load flow equations are associated with the various network elements, including the coupling node. Collecting all the equations gives the integrated system of equations for steady-state load flow of a MES. This new framework makes it possible to describe integrated energy systems in a very efficient way.

The proposed framework includes and extends the currently available load flow models for MES. It provides guidelines for combining SC gas, electricity, and heat networks into one MCN, such that the resulting integrated system of load flow equations is (uniquely) solvable. Our coupling nodes are very general. Therefore, it is possible to represent a large variety of coupling components, and to use various models for (the same) coupling components, both linear and nonlinear. The coupling nodes in this paper are able to describe bidirectional flow in a correct way. The framework can be used for MES including other carriers than gas, electricity, or heat.

In short, our main contributions are: (i) the generic, uniform representation of energy transportation networks, (ii) the use of coupling nodes to couple energy networks, allowing for easy integration of various single-carrier networks into MCNs, and (iii) insight into existence and uniqueness of solutions of integrated load flow problems.

In Section 2, we present our comprehensive graph representation of MESs consisting of gas, electricity and heat. The load flow models and coupling models for the various network elements are described in Section 3. We propose an integrated steady-state load flow model for MESs in Section 4. In this section, the need for additional BCs, and the effect on the integrated system of load flow equations is described. In Section 5, an example MES is used for validation, and to provide insight into solvability issues due the coupling of the SCNs into one MCN.

2. Graph representation

Energy systems have their own terminology based on the energy carrier. For instance, a basic power grid is an electrical network consisting of power lines connected by buses, whereas a basic gas network consists of pipes connected at junctions. Mathematically, all energy systems are represented by a graph or network.

2.1. Terms and definitions

A graph is a pair (,), where is a set of nodes or vertices v_i and is a set of links or edges e_k. A link is a set of two nodes, $e_k = \{v_i, v_j\}$, or an ordered pair of nodes, $e_k = (v_i, v_j)$. If all links in are ordered, the graph is directed, if none of the links are ordered, the graph is undirected. A network is a graph, directed or not, with an associated physical model. An energy transportation network, or flow network, is a network where the associated model is a representation of an energy transportation system, in which energy is transported along the links.

Flow enters or leaves the network through sources and sinks, which are both called loads or terminal nodes. In the graph, these terminal nodes are a subset of . Inflow and outflow can be represented by values associated with the terminal nodes, but it is convenient to see inflow and outflow of a terminal node as flow through an open link connected to that node. These open links, connected to a single node only, are called terminal links. By definition, a terminal link can only be connected to a terminal node. Conversely, a node without a terminal link connected to it is not a terminal node. The direction of a terminal link is defined as outgoing, such that the terminal node acts as a source if the flow is opposite in direction to the terminal link, and acts as a sink if the flow is in the same direction as the terminal link. We add the terminal links explicitly to the network representation.

Let be the set of terminal links. Then a flow network is represented by the collection = { , , } = { , }. Hence, is directed if is directed, and undirected if is undirected.

For notational simplicity, i is used as the node index (v_i), k as the link index (e_k), and l as the terminal link index (t_l).

2.2. Single-carrier energy systems

A gas network is represented by a directed graph. A node represents

a junction, sink, or source, where a junction is modeled as a terminal node with zero in- or outflow. A pipe or a compressor is represented by a link. A balanced alternating current (AC) power grid is represented by an undirected graph. A node represents a bus, sink, or source. A transmission line or a transformer is represented by a link. The physical pipeline model of a heat pipeline system consists of a supply line and return line, connected to each other through the (heat) loads. Heat is injected into or extracted from the water in the network through heat exchangers (see e.g. [13]). A circulation pump is usually located at the source of the heating system. Hence, the hydraulic part of the heat network is a closed system. Fig. 1a gives a model representation of a source connected to a sink by a single pipe. We assume that the water flow in the return line is opposite in direction, but equal in size, to the water flow in the supply line [14]. The return line is not modeled explicitly, and the hydraulic part of the system is no longer closed. A heat pipeline system is then represented as a directed graph. A node represents a junction, sink, or source. A pipe in the supply line is represented by a link. A terminal link represents a heat exchanger and a connection between supply and return line. We assume that a node can have only sink or only source terminal links connected to it, such that we can call the node a sink or a source respectively. Fig. 1b gives the network representation of a source connected to a sink by a single pipe.

Variables are associated with nodes, links, and terminal links. For basic steady-state load flow analysis, these variables, and the network elements they are associated with, are shown in Table 1. Variables associated with terminal links are seen as nodal variables. To distinguish between (terminal) link and nodal variables, the nodal variables are called injected. If a node has more than one terminal link connected to it, the injected flow or power is the sum of all the flows or powers on the terminal links. For the load flow equations, some nodal and links variables are associated with the beginning or end of a link, directly next to a node. For a link from node i to node j, they are denoted by $[\cdot]_{ij}^{\text{start}}$ and $[\cdot]_{ij}^{\text{end}}$ respectively. See for example the supply and return line temperatures of the heat network in Fig. 1b. For pipe models, it typically holds that $q_{ij} = -q_{ji}$, with gas flow q, or $m_{ij} = -m_{ji}$, with water flow m, whereas for most electrical line models $I_{ij} \neq -I_{ji}$, with complex current I.

2.3. Coupling of energy systems

Two nodes can be connected in three ways: connect the two nodes by a link, merge the two nodes into one node, or introduce an additional node and connect the nodes to it. A link is a network component with two flow connections, making it difficult to use as a representation of a coupling involving more than two carriers, such as a combined heat and power plant (CHP). Moreover, a physical interpretation of a coupling link is not straightforward. Coupling by merging two nodes is complicated by the nodal variables. Suppose we want to merge two electrical nodes, each with a voltage magnitude $|V|$ and voltage angle δ, into one new electrical node. Some combined $|V|$ and δ must then be defined for this new node, or a node with multiple voltages must be allowed. Coupling two nodes of a different carrier by merging introduces similar difficulties. Therefore, we couple networks by introducing an additional node, called a coupling node.

No variables are associated with the coupling node, meaning that it does not belong to any of the SCNs. If the coupling node is used to couple networks with the same carrier, the coupling node is called homogeneous. Similarly, it is called heterogeneous when used to couple networks with different carriers. Nodes and links of an SCN are called homogeneous. A network is then called heterogeneous if it has one or more heterogeneous nodes, and homogeneous if it consists of only homogeneous nodes and links. A heterogeneous coupling node can be connected to a (terminal) link of any carrier. However, no variables are associated with the coupling node, so that links representing certain physical components cannot be connected. For instance, a link representing a gas pipe cannot be connected, since the flow model associated with the link requires both start and end node to have a nodal pressure p. We couple a (heterogeneous) coupling node to any other node by a dummy link. These links do not represent any physical component, they merely show a connection between nodes. If the dummy link connects a coupling node and a SC node, the dummy link is considered homogeneous and of the same carrier as the SC node. As such, it has the same variables associated with it as any other link of that carrier. Fig. 2 shows the network representation of a heterogeneous coupling node connecting a gas network, electrical network, and heat network. The arrows on the (terminal) links show defined directions, not actual directions of flow. Hence, the coupling node concept allows for bidirectional flow.

3. Load flow models

Conservation of energy holds for all the SC nodes. All SC links representing a physical component have a link equation, which relates link and nodal variables, determined by the physical component. The general equations per carrier and network element are given as follows.

3.1. Gas

For steady-state load flow, a basic gas network can be completely described by conservation of mass and the link equations [15]. In every node $v_i \in {}^{g}$, conservation of mass holds:

$$f_i^q := \sum_{j,j\neq i} q_{ij} - q_i = 0 \tag{1}$$

with q_i the injected flow, and q_{ij} the link flow. For every link $e_k \in {}^{g}$ from node $v_i \in {}^{g}$ to node $v_j \in {}^{g}$, the general link equation is given by:

$$f_k^g\left(q_{ij}, p_i^g, p_j^g\right) = 0 \tag{2}$$

with p_i^g the nodal pressure. For gas pipes, the link equations are generally nonlinear in the pressures.

3.2. Electricity

Using an AC steady-state approximation, a power grid is completely

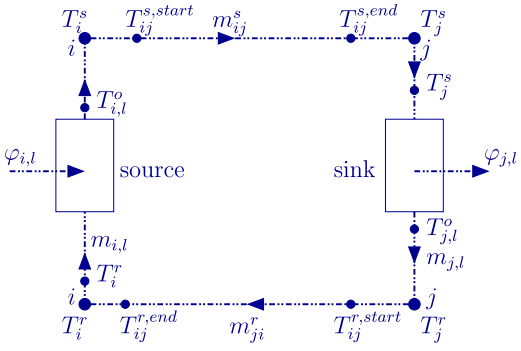

(a) Model representation.

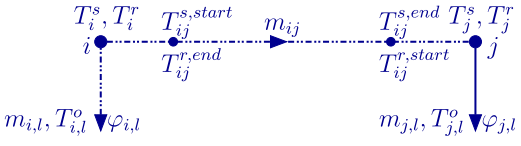

(b) Network representation.

Fig. 1. Model (a) and network (b) representation of a heating system consisting of a source i connected with a single pipe to a sink j. Variables are shown next to the element they are associated with (see Table 1). Terminal links are defined as outgoing.

Table 1
Load flow variables for a gas, heat, and electrical network, per associated network element.

Carrier	Node	Link	Terminal node
Gas	Pressure p^g	Flow q	Injected flow q
Heat	Pressure p^h	Flow m	Injected flow m
	Supply temperature T^s		Outflow temperature T^o
	Return temperature T^r		Heat power φ
Electricity	Voltage V	Current I	Injected current I
			Injected complex power S

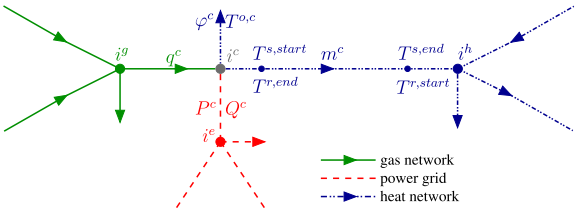

Fig. 2. Coupling node i^c, connected by dummy links to a gas node i^g, an electrical node i^e, and a heat node i^h. The coupling variables are shown next to the (terminal) links they are associated with.

described by Kirchhoff's current law, link equations, and the complex power equation [16]. In every node $v_i \in$ ^{e}, Kirchhoff's current law holds:

$$f_i^I := \sum_{j,j\neq i} I_{ij} - I_i = 0 \tag{3}$$

with I_i the injected current, and I_{ij} the link current. For every link $e_k \in$ ^{e} from node $v_i \in$ ^{e} to node $v_j \in$ ^{e}, the general link equation is given by:

$$f_k^e(I_{ij}, V_i, V_j) = 0 \tag{4}$$

with V_i the nodal voltage. Finally, in every node $v_i \in$ ^{e}, the complex power equation holds:

$$f_i^S := S_i - V_i(I_i)^* = 0 \tag{5}$$

with S_i the injected complex power, and where $[\cdot]^*$ denotes the complex conjugate.

3.3. Heat

The load flow model for a heat network consists of a hydraulic and a thermal part. Using a steady-state approximation, the hydraulic part is similar to the model for a gas network, such that conservation of mass holds in every node $v_i \in$ ^{h}, and a link (flow) equation holds for every link $e_k \in$ ^{h} from node $v_i \in$ ^{h} to node $v_j \in$ ^{h}. The thermal part is completely described by conservation of energy, a thermal link equation, and the heat power equation. In every node $v_i \in$ ^{h}, conservation of mass holds:

$$f_i^m := \sum_{j,j\neq i} m_{ij} - m_i = 0 \tag{6}$$

with m_i the injected mass flow, and m_{ij} the link mass flow. For every link $e_k \in$ ^{h} from node $v_i \in$ ^{h} to node $v_j \in$ ^{h}, the general hydraulic link equation is given by:

$$f_k^h\left(m_{ij}, p_i^h, p_j^h\right) = 0 \tag{7}$$

with p_i^h the nodal pressure. For heat pipes, the link equations are generally nonlinear in the mass flow. The general thermal link equations are given by:

$$\begin{aligned} f_k^{s,\psi}(T_k^{s,\text{start}}, T_k^{s,\text{end}}, m_k) &= 0 \\ f_k^{r,\psi}(T_k^{r,\text{start}}, T_k^{r,\text{end}}, m_k) &= 0 \end{aligned} \tag{8}$$

with T^s the supply line temperature, and T^r the return line temperature. The 'start' and 'end' of the link are defined with respect to actual direction of flow instead of defined direction of the link. In every node $v_i \in$ ^{h}, conservation of energy holds. Assuming a constant specific heat C_p of the water, and only taking convection within the water into account, it reduces to a mixing-rule:

$$\begin{aligned} f_i^{T^s} &:= (\sum m_{\text{out}}^s)T_i^s - \sum(m_{\text{in}}^s T_{\text{in}}^s) = 0 \\ f_i^{T^r} &:= (\sum m_{\text{out}}^r)T_i^r - \sum(m_{\text{in}}^r T_{\text{in}}^r) = 0 \end{aligned} \tag{9}$$

where $\sum m_{\text{out}}$ denotes the sum of all outgoing flows of node v_i. Note that $\sum m_{\text{in}}^r = \sum m_{\text{out}}^s$ and $\sum m_{\text{out}}^r = \sum m_{\text{in}}^s$. A heat source or sink, represented by a terminal link t_l connected to node v_i, has a heat power equation given by:

$$f_{i,l}^{\varphi} := C_p m_{i,l} \Delta T_{i,l} - \varphi_{i,l} = 0 \tag{10}$$

with a temperature difference defined by:

$$\Delta T_{i,l} := \begin{cases} T_i^s - T_{i,l}^o & \text{,if } t_l \text{ is a sink} \\ T_{i,l}^o - T_i^r & \text{,if } t_l \text{ is a source} \end{cases} \tag{11}$$

Here, $\varphi_{i,l}$ is the heat power, $m_{i,l}$ is the mass flow of the terminal link, and $T_{i,l}^o$ is the outflow temperature of the source or sink. Since a terminal link is defined as outgoing, $\varphi_{i,l},\ m_{i,l} > 0$ if t_l is a sink, and $\varphi_{i,l},\ m_{i,l} < 0$ if t_l is a source.

3.4. Multi-carrier energy systems

To create a MES, homogeneous nodes are coupled to a heterogeneous coupling node using dummy links. The dummy links only show a connection between nodes, they do not represent a physical component. However, they could be seen as lossless transmission lines or pipes for model purposes. A gas dummy link only has a gas flow q_k, but no link equation. An electrical dummy link has complex current $I_{ij} = -I_{ji}$, active power $P_{ij} = -P_{ji} := -P$, and reactive power $Q_{ij} = -Q_{ji} := -Q$, but no link equation, such that P and are independent of V and I. A heat dummy link has mass flow m_k, supply temperature $T_{ij}^{s,\text{start}} = T_{ij}^{s,\text{end}}$, and return temperature $T_{ij}^{r,\text{start}} = T_{ij}^{r,\text{end}}$. The coupling variables, denoted by $[\cdot]^c$, and their associated location in the network representation are shown in Fig. 2. Since the dummy links are homogeneous links, their variables contribute to the nodal equations of the homogeneous nodes they are connected to.

In every heterogeneous coupling node $v_i \in$ ^{c}, one or more coupling equations hold. For a node i connected with a dummy link to a homogeneous node j of each carrier, and connected with one heat terminal link l, we assume the coupling equations to be of the general form:

$$f_i^c\left(q_{ij}^c, P_{ij}^c, Q_{ij}^c, m_{ij}^c, T_{ij}^s, T_{ij}^r, m_{i,l}^c, T_{i,l}^{o,c}, \varphi_{i,l}^c\right) = 0 \tag{12}$$

This general form can be easily adjusted if a coupling node has multiple or no links of a carrier connected to it. Since a heat terminal link represents a heat source or sink, one of the coupling equations will be a heat Eq. (10) for every heat terminal link connected to the coupling node.

Any physical coupling unit for which the model equation(s) are of the form (12), can be represented by a (heterogeneous) coupling node. Most conversion units, such as gas-fired generators, CHPs, electrical boilers, or gas-to-power units are modeled in such a way. Moreover, the coupling node concept allows for both linear and nonlinear models.

4. System of equations

4.1. Node types

Typically, the SCNs have more variables than equations. Therefore, some (nodal) variables are assumed known, which we call the boundary conditions (BCs) of the network. A node type is assigned to every node based on the known variables. The standard node types for SCNs are shown in Table 2. The steady-state load flow problem is formulated by collecting the load flow equations into one system of equations. The size of this system for the SCNs is reduced by using the BCs and by substituting some equations into others. For each carrier, several formulations for the system of equations are used, see e.g. [15] for gas, [16,17], or [18] for electricity, and [9] or [19] for heat. We use the following systems of equations.

For gas, we use the full formulation (instead of the more commonly used nodal formulation). The system of (nonlinear) equations is given by:

$$\boldsymbol{F^g} = \begin{pmatrix} \boldsymbol{F^q} \\ \boldsymbol{F^L} \end{pmatrix} = \boldsymbol{0}, \quad \boldsymbol{x^g} = \begin{pmatrix} \boldsymbol{q} \\ \boldsymbol{p^g} \end{pmatrix} \tag{13}$$

with $\boldsymbol{p^g}$ the vector of unknown nodal pressures, $\boldsymbol{q}$ the vector of unknown link flows, $\boldsymbol{F^q}$ the vector of conservation of mass (1) for every node with known injected flow, and $\boldsymbol{F^L}$ the vector of link equations.

For electricity, we use the complex power formulation in polar coordinates. For every node i, the link Eqs. (4) are substituted in Kirchhoff's current law (3), which is subsequently substituted in the complex power Eq. (5). This equation, which gives conservation of energy, is then split in the active power part f_i^P and reactive power part f_i^Q, where $f_i^S = f_i^P + \mathrm{i} f_i^Q$. The system of (nonlinear) equations is given by:

$$\boldsymbol{F^e} = \begin{pmatrix} \boldsymbol{F^P} \\ \boldsymbol{F^Q} \end{pmatrix} = \boldsymbol{0}, \quad \boldsymbol{x^e} = \begin{pmatrix} \boldsymbol{\delta} \\ \boldsymbol{|V|} \end{pmatrix} \tag{14}$$

Here, $\boldsymbol{F^P}$ and $\boldsymbol{F^Q}$ are the vectors of conservation of energy for every node with known injected active or reactive power, and $\boldsymbol{\delta}$ and $\boldsymbol{|V|}$ are the vectors of unknown nodal voltage angle and voltage amplitude.

For heat, the thermal link Eqs. (8) can usually be rewritten such that T_k^{end} is a function of m_k and T_k^{start}. This temperature is then substituted in the mixing-rule (9). We consider two different BCs for the terminal links, we assume $\varphi_{i,l}$ and either $T_{i,l}^o$ or $\Delta T_{i,l}$ known. If T^o is known, it is substituted in (9) and in (10). If instead $\Delta T_{i,l}$ is known, $T_{i,l}^o$ is added as a variable, and (11) is added to the system of equations as

$$0 = f_{i,l}^{\Delta T} = \begin{cases} T_i^s - T_{i,l}^o - \Delta T_{i,l} & \text{,if } l \text{ is a sink} \\ T_{i,l}^o - T_i^r - \Delta T_{i,l} & \text{,if } l \text{ is a source} \end{cases} \tag{15}$$

In the commonly used formulation (see e.g. [5] or [9]), the terminal flows $m_{i,l}$ are written as function of $T_{i,l}^o$ and $\varphi_{i,l}$, using (10), and substituted into the other equations. The resulting system of equations is smaller than (16). However, conservation of mass (6) is then nonlinear, and the supply line mixing rule f^{T^s} depends on T^r and vice versa. We do not substitute terminal flows into the other equations. The system of nonlinear equations for this terminal link formulation is then given by:

$$F^h = \begin{pmatrix} F^m \\ F^L \\ F^{T^s} \\ F^{T^r} \\ F^{\varphi} \\ F^{\Delta T} \end{pmatrix} = 0, \quad x^h = \begin{pmatrix} m^L \\ m^{TL} \\ p^h \\ T^s \\ T^r \\ T^o \end{pmatrix} \tag{16}$$

with m^L the vector of link mass flows, m^{TL} the vector of unknown terminal link mass flows, p^h the vector of unknown nodal pressures, T^s and T^r the vectors of unknown nodal supply and return temperatures, T^o the vector of unknown terminal outflow temperatures, F^m the vector of conservation of mass for every non slack node, F^L the vector of link equations, F^{T^s} the vector of supply line mixing rules for every node with T_i^s unknown and every source node with $T_{i,l}^o$ unknown, F^{T^r} the vector of return line mixing rules for every node with T_i^r unknown and every sink node with $T_{i,l}^o$ unknown, F^{φ} the vector of heat power equations, and $F^{\Delta T}$ the vector of temperature difference equations.

For an MCN, the dummy and terminal links of a coupling generally introduce more variables than the coupling node introduces equations. These extra degrees of freedom could be used for optimization purposes (e.g. [20]). However, for steady-state load flow, (additional) BCs are needed in an MCN. One commonly used option is to prescribe one or more of the coupling energies (e.g. [2,5,10,12]). However, this effectively decouples the integrated network. If one or more of the coupling energies are known, the coupling equations of most coupling units can be used to directly determine (some of) the other energies. These energies, combined with the already prescribes ones, can then be used as BCs for the SCNs. In that case, there is no need to model the load flow problem as one integrated system of equations, and the advantages provided by a coupling are not fully used. Therefore, we will assume all coupling (energy) flows, q^c, P^c, Q^c, m^c, and φ^c, unknown. If a coupling unit produces or consumes heat, $T^{o,c}$ or ΔT^c can be assumed known as a BC without decoupling the system of equations. The additionally required boundary conditions are imposed elsewhere in the MCN, that is, they are imposed in the single-carrier parts.

Imposing the additionally required BCs on the homogeneous nodes may lead to new node types, as also observed in [7] for a power grid. Consider, for instance, a gas network connected to a power grid through a generator. Suppose the electrical node to which we couple is a slack node before coupling, such that P and are unknown, and $|V|$ and δ are known. We could then replace this unknown input power with the unknown coupling power, such that the coupling, or the gas network, could be considered as the slack for the power grid. However, the coupling powers P^c and Q^c flow into the power grid through a dummy link. Since we want to replace the slack powers with the coupling powers, the total injected power of the electrical node should be zero after coupling. Hence, the electrical node turns into a new node with P, Q, $|V|$, and δ known, called a PQVδ-node. Table 3 gives some, but not all, possible new node types. The names of the node types indicate which variables are assumed known. For the heat network, nodes that are not a sink or a source are junctions, which are nodes that have no inflow or outflow. In the physical heating system, these corresponds to junctions in the pipelines, without a connection between the supply and the return line. Not all of these are realistic from a physical perspective. For instance, a heat sink slack node would physically be a node where the pump to regularize pressure is located at a sink instead of at a source. However, they might be needed to solve the integrated system of equations.

The system of nonlinear equations for the coupling part is given by:

Table 2
Standard node types for single-carrier networks.

Network	Node type	Specified	Unknown
Gas	Reference	p^g	q
	Load	q	p^g
Electricity	Slack	$\|V\|$, δ	P, Q
	Generator (PV)	P, $\|V\|$	Q, δ
	Load (PQ)	P, Q	$\|V\|$, δ
Heat	Source reference slack	T^s, p^h	T^r, T^o, φ, m
	Source	T^o and $\varphi < 0$	T^r, T^s, p^h, m
	Sink	T^o and $\varphi > 0$	T^r, T^s, p^h, m
	Junction	$m = 0$	T^r, T^s, p^h

Table 3
Some possible new node types for multi-carrier networks.

Carrier	Node type	Specified	Unknown
Gas	Slack	–	p^g, q
	Reference load	p^g, q	–
Electricity	PVδ	P, $\lvert V\rvert$, δ	Q
	QVδ	Q, $\lvert V\rvert$, δ	P
	PQVδ	P, Q, $\lvert V\rvert$, δ	–
Heat	Source/sink reference	T^o, φ, p^h	T^s, T^r, m
	Source temperature	T^s, T^o, and $\varphi < 0$	T^r, p^h, m
	Reference	p^h, $m = 0$	T^r, T^s
	Temperature	T^s, $m = 0$	T^r, p^h
	Reference temperature	T^s, p^h, $m = 0$	T^r
	Sink slack	T^r, p^h	T^s, T^o, φ, m
	Source/ sink ΔT	ΔT, φ	T^o, T^r, T^s, p^h, m
	Source/sink reference ΔT	ΔT, φ, p^h	T^o, T^r, T^s, m
	Source temperature ΔT	ΔT, T^s, φ	T^o, T^r, p^h, m
Coupling	Standard	–	T^o
	Temperature	T^o	–
	ΔT	ΔT	T^o

$$F^c = \begin{pmatrix} f^c \\ F^{\varphi^c} \\ F^{\Delta T^c} \end{pmatrix} = 0, \quad x^c = \begin{pmatrix} q \\ P \\ Q \\ m \\ \varphi \\ T^o \end{pmatrix} \tag{17}$$

Here, f^c is the vector of coupling equations, F^{φ^c} is the vector of heat power equations, $F^{\Delta T^c}$ the vector of temperature difference equations, T^o is the vector of unknown outflow temperatures, and q, P, Q, m, and φ are the vectors of the coupling gas flow, active power, reactive power, water link mass flow, and terminal link heat power.

The load flow equations of the SC parts and the coupling part are combined to form the integrated system of nonlinear equations describing the steady-state load flow problem for a MES. Since a (heterogeneous) coupling node is connected by homogeneous (dummy) links to the homogeneous single-carrier nodes, q^c, P^c, Q^c, and m^c are included in the nodal conservation laws of the SCNs. Furthermore, m^c and $T^{o,c}$ are included in (9) of the heat network, and $T^r_{i^h}$ is included in the heat power equation for the coupling node, if the coupling unit produces heat. Combining the SC systems (13), (14), and (16) with the coupling part (17) gives the integrated system of equations for a MES:

$$F = \begin{pmatrix} F^g \\ F^e \\ F^h \\ F^c \end{pmatrix} = 0, \quad x = \begin{pmatrix} x^g \\ x^e \\ x^h \\ x^c \end{pmatrix} \tag{18}$$

4.2. Scaling

The variables and parameters in the load flow equations can have values which are orders of magnitude apart, even within an SCN. For instance, usually $q \sim 1$ kg/s whereas $p^g \sim 10^5$ Pa. Normalizing or scaling the variables and equations for power grids is commonly done, and is called the per unit system (e.g. [16]). In [5], this system is extended to the heat network, to have consistency throughout the MES. We extend this notion further, such that a per unit system can be adopted in the gas network as well. The per unit value of a quantity x is defined as:

$$x_{\text{p.u.}} := \frac{x_a}{x_b} \tag{19}$$

with x_a the actual value and x_b the base value. The per unit value is dimensionless, but is usually given dimension p.u.. For a power grid, $\lvert V\rvert_b$ and $\lvert S\rvert_b$ are usually given. The other base values, assuming single-phase flow, are then determined by:

$$\begin{aligned} \lvert I\rvert_b &= \frac{\lvert S\rvert_b}{\lvert V\rvert_b} \\ \lvert y\rvert_b &= \frac{\lvert S\rvert_b}{\lvert V\rvert_b^2} \end{aligned} \tag{20}$$

with y the admittance. In the per unit system, the same load flow Eqs. (3)–(5) are used as in the unscaled case, but with the normalized parameters and variables. For gas, we specify q_b and p^g_b. The parameters in the load flow Eqs. (1) and (2) are determined based on q_b and p^g_b, such that (1) and (2) hold for both the actual and the per unit variables. For a heat network, we specify m_b, p^h_b, T_b, and φ_b, and the parameters in the load flow equations are determined accordingly.

For many coupling units, generally $E^{g,c} \sim P^c \sim \varphi^c$ with $E^g := \text{GHV}q$ and GHV the gross heating value of gas. Hence we take $E^{g,c}_b = \varphi^c_b = \lvert S\rvert_b$ for consistency throughout the MES. The parameters in the coupling Eq. (12) are determined accordingly, based on $E^{g,c}_b$, P^c_b, and φ^c_b, such that (12) holds for both the actual and the per unit variables.

The per unit system requires scaling all parameters in every equation used. Another option is to scale F and x by matrix multiplication. The equations are scaled by a diagonal matrix D_F with $(D_F)_{nn} = \frac{1}{(F_b)_n}$, with F_b the vector with base values for each equation, such that $\hat{F} := D_F F$ is the scaled system of equations. The variables are scaled by a diagonal matrix D_x with $(D_x)_{nn} = \frac{1}{(x_b)_n}$, with x_b the vector with base values for each variable, such that $\hat{x} := D_x x$ is the scaled variable vector. The base values for the load flow equations are chosen such that $(F_a)_n = (F_b)_n (F_{\text{p.u.}})_n$ for every n. Then $F_{\text{p.u.}} = D_F F_a$ and $x_{\text{p.u.}} = D_x x_a$. Hence, using D_F and D_x with suitable base values is equivalent to using the per unit system, without having to scale all the parameters in every equation used.

4.3. Newton–Raphson method

Several methods can be used to solve a nonlinear system of equations. For instance, fixed-point iteration methods, such as the Gauss–Seidel power flow method for power grids, or the Newton–Raphson method (NR). We solve the integrated system of nonlinear Eq. (18) using NR, because it has quadratic convergence. The iteration scheme in multiple dimensions is given by:

$$J(x^k)s^k = -F(x^k) \tag{21a}$$

$$x^{k+1} = x^k + s^k \tag{21b}$$

Due to the choice for a (heterogeneous) coupling node connected to the SCNs by (homogeneous dummy) links, the Jacobian matrix J is given by:

$$J = \begin{pmatrix} J^{gg} & J^{ge} & J^{gh} & J^{gc} \\ J^{eg} & J^{ee} & J^{eh} & J^{ec} \\ J^{hg} & J^{he} & J^{hh} & J^{hc} \\ J^{cg} & J^{ce} & J^{ch} & J^{cc} \end{pmatrix} = \begin{pmatrix} J^{gg} & 0 & 0 & J^{gc} \\ 0 & J^{ee} & 0 & J^{ec} \\ 0 & 0 & J^{hh} & J^{hc} \\ 0 & 0 & J^{ch} & J^{cc} \end{pmatrix} \tag{22}$$

where the submatrices are defined as

$$J^{\alpha\beta} = \frac{\partial F^\alpha}{\partial x^\beta}, \quad \alpha, \beta \in \{g, e, h, c\} \tag{23}$$

This distinct structure holds for any MCN for which the load flow equations satisfy the general form (1)–(12). Since the BCs additionally required by the coupling are imposed in the SC parts, these submatrices will generally not be square. In other words, a single-carrier part might be overdetermined while another might be underdetermined. Moreover, without reordering, this system (21a) cannot be solved blockwise.

When using scaling by matrix multiplication, the iteration scheme is adjusted to [21]:

$$\hat{\mathrm{J}}(x^k)\hat{s}^k = -\hat{F}(x^k) \tag{24a}$$

$$\hat{x}^{k+1} = \hat{x}^k + \hat{s}^k \tag{24b}$$

with $x^k = D_x^{-1}\hat{x}^k$, and $\hat{\mathrm{J}}(x^k) = D_F J(x^k) D_x^{-1}$. Note that $J_{\mathrm{p.u.}} = D_F J_a D_x^{-1}$ when D_F and D_x are chosen such that $F_{\mathrm{p.u.}} = D_F F_a$ and $x_{\mathrm{p.u.}} = D_x x_a$. Therefore, unscaled NR (21) with the per unit system is equivalent to scaled NR (24).

For the error e^k at each NR iteration k, we use $e^k = ||F(x^k)||_2$ for unscaled NR (21), and $e^k = ||D_F F(x^k)||_2$ for scaled NR (24), with $||\cdot||_2$ the 2-norm. Convergence is reached after k iterations if $e^k < \mathrm{tol}$ for a chosen tolerance tol.

In general, it is difficult to derive conditions to guarantee convergence, both for fixed-point methods and for NR. If the problem is ill-posed, such that the Jacobian matrix is singular, NR will not find a solution, even if the initial guess x^0 is close to the solution. Even if the problem is well-posed, care has to be taken when initializing the solution vector. A badly chosen initial guess can cause convergence problems for the solver. Moreover, it can lead to singular Jacobians, depending on the models used. For instance, a well-known problem in gas networks is the zero-flow problem, where a zero flow rate in a pipe can cause zero first derivatives of flow equations, and hence singular Jacobians. Other commonly used pipe flow models can cause zero or undefined first derivatives of the flow equations for a flat initial guess of pressure. The models used for the gas and heat pipes in the examples in Section 5 require nonzero flow, but can handle a flat pressure field.

4.4. Model framework

The proposed graph-based model framework for steady-state load flow problems of MES is summarized as follows, which is also shown in Fig. 3. First, the SCs gas, electricity, and heat systems to be combined into a multi-carrier system are represented by a network as described in Section 2.2. Then, the desired coupling units are represented by a coupling node, and connected to SC networks using dummy links, as described in Section 2.3. The resulting graph is the MCN corresponding to the MES. Third, load flow equations are chosen for each network element, see Section 3. Node types, or BCs, are chosen, and the load flow equations are collected into one integrated system of Eqs. (18). Finally, this system of nonlinear equation is solved using NR.

The node types, and the location of the coupling nodes in the graph, must be carefully chosen. Certain combinations of node types, or graph topologies, can result in systems of equations that are not (uniquely) solvable. A necessary condition for the load flow problem to be uniquely solvable is that the number of equations F is equal to the number of variables x. However, even with a square system, the problem might still be ill-posed, such that are no or multiple solutions. The proposed model framework provides insight into when the load flow problem of a MES is uniquely solvable [22].

Using dummy links to connect the SC into one MCN show the connection between the SC parts explicitly. This connection is more difficult to see when the coupling flows are incorporated into injected nodal flows, as is commonly done (see for instance [5,10], or [12]). Furthermore, using dummy links, the load flow models of the SC parts are only slightly altered, and the effect of coupling is included through the coupling part of the system of equations, as reflected by the distinct structure of the Jacobian matrix (22).

The load flow models and network elements can represent a variety of physical components of an energy system, such that the model framework is applicable to general MESs. Moreover, using different coupling components, models, or node types, results in different MCNs for the same MES.

5. Example

To illustrate the proposed model framework, we consider a small MES, which is based on a case study introduced in [10], and later adapted in [5] using an extended EH approach. For comparison, and to show that our framework is applicable to general MES, we consider two different ways of coupling the single-carrier networks of this MES, one similar to the couplings used in [10] and the other similar to [5].

5.1. Networks

Fig. 4a and b show the networks for both ways of coupling. In network 1, we use a gas-fired generator (GG), gas boiler (GB), and a combined heat and power plant (CHP) for the coupling. In network 2, we use two EHs. For both networks, the same models are used in the single-carrier part. We use the models given below. All equations, variables, and parameters are in S.I. units, unless stated otherwise. Table 4 summarizes the parameter values used in the equations for both networks.

In the gas network, links $0^g - 1^g$, $0^g - 2^g$, and $3^g - 2^g$, represent pipes, and link $1^g - 2^g$ represents a compressor. The pipes are modeled using the steady-state flow equation (e.g. [15]), such that the link Eq. (2) becomes

$$f_k^g\left(q_{ij}, p_i^g, p_j^g\right) = \Delta p_k^g - \frac{f_k}{C_k^{g^2}} q_k \left| q_k \right| = 0 \tag{25}$$

with $\Delta p_k^g = (p_i^g)^2 - \left(p_j^g\right)^2$, f_k the Fanning friction factor, and C_k^g the pipe constant:

$$C_k^g = \frac{\pi}{8}\sqrt{\frac{SD_k^5}{TR_{\mathrm{air}}L_k Z}} \tag{26}$$

with S the specific gravity of the gas, R_{air} the specific gas constant of air, T the temperature of the gas, Z the compressibility factor, D_k the pipe diameter, and L_k the pipe length. For the friction factor, we use the implicit Colebrook-White equation for the turbulent regime:

$$\frac{1}{2\sqrt{f_k}} = -2\log_{10}\left(\frac{\epsilon_k}{3.7D_k} + \frac{2.51}{\mathrm{Re}\sqrt{f_k}}\right) \tag{27}$$

with ϵ_k the relative roughness of the pipe, $\mathrm{Re}=\frac{4q_k}{\pi\mu\rho_n D_k}$ the Reynolds number, with μ the kinematic viscosity, and $\rho_n = (p_n S)/(R_{\mathrm{air}}T_n)$ the density of the medium at standard conditions with T_n the temperature at standard conditions. The compressor is modeled by a fixed pressure ratio, such that the link Eq. (2) becomes

$$f_k^g\left(p_i^g, p_j^g\right) = r_k p_i^g - p_j^g = 0 \tag{28}$$

with r_k the compressor ratio.

In the electrical network, all links represent transmission lines, which we model as short lines. The power in the links is then given by (e.g. [16]):

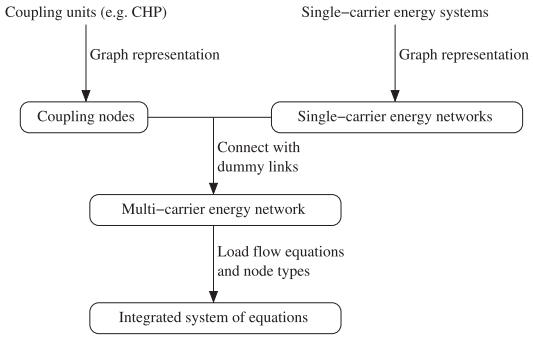

Fig. 3. Flowchart of the graph-based model framework for steady-state load flow problems of MESs.

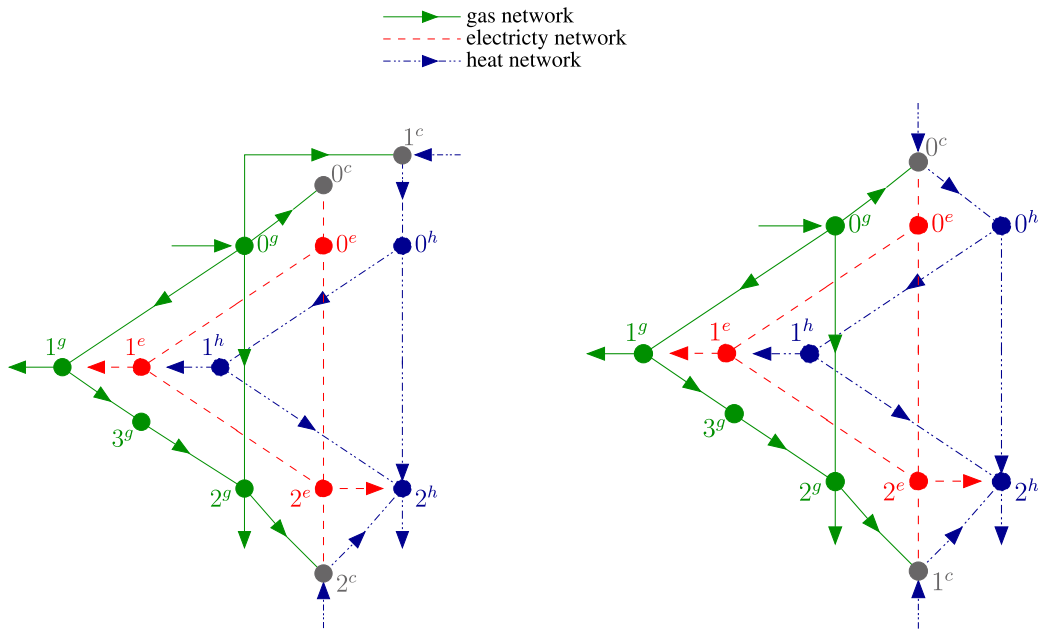

(a) Network 1. (b) Network 2.

Fig. 4. Network topology using two different ways of coupling. Network 1 (a) is based on [10], network 2 (b) is based on [5]. The links show predefined direction of flow, the terminal links show actual direction of flow.

$$\begin{aligned} P_{ij} &= g_{ij}\left|V_i\right|^2 - \left|V_i\right|\left|V_j\right|\left(g_{ij}\cos\delta_{ij} + b_{ij}\sin\delta_{ij}\right) \\ Q_{ij} &= -b_{ij}\left|V_i\right|^2 - \left|V_i\right|\left|V_j\right|\left(g_{ij}\sin\delta_{ij} - b_{ij}\cos\delta_{ij}\right) \end{aligned} \tag{29}$$

with $y_{ij} = g_{ij} + \imath b_{ij}$ the line admittance. Using these link equations, the complex power Eq. (5) for a node i then becomes

$$\begin{pmatrix} f_i^P \\ f_i^Q \end{pmatrix} = \begin{pmatrix} \sum_{j,j\neq i} P_{ij} - P_i \\ \sum_{j,j\neq i} Q_{ij} - Q_i \end{pmatrix} = 0 \tag{30}$$

We use $x_{ij} = 1/6\ \Omega$and $r_{ij} = x_{ij}/10$ for all links. The admittance is the inverse of the line impedance $z_{ij} = r_{ij} + \imath x_{ij}$, such that $b_{ij} = -x_{ij}/|z_{ij}|^2$ and $g_{ij} = r_{ij}/\left|z_{ij}\right|^2$.

In the heat network, all links represent pipes. For the hydraulic model, we use a steady-state flow equation, such that the link Eq. (7) becomes

$$f_k^h\left(m_{ij}, p_i^h, p_j^h\right) = \Delta p_k^h - \frac{f_k}{C_k^{h^2}}\left|m_k\right|m_k = 0 \tag{31}$$

with $\Delta p_k^h = p_i^h - p_j^h$, and C_k^h the pipe constant:

$$C_k^h = \frac{\pi}{8}\sqrt{\frac{2\rho D_k^5}{L_k}} \tag{32}$$

with ρ the density of the water, D_k the diameter of the pipe, and L_k the length of the pipe. We use the friction factor given by Colebrook-White's Eq. (27). For the thermal model in both supply and return line, we assume that the convective heat transfer from the water into the surroundings is in the radial direction only, that the heat loss of a pipe is independent of the direction of flow, and that the conductive heat transfer within the water is negligible. The temperature drop over a pipe then becomes exponential [23], such that the thermal link Eq. (8), for both the supply and return line, is given by

$$T_k^{\text{end}} = \exp\left(\frac{-\lambda_k L_k}{C_p|m_k|}\right)\left(T_k^{\text{start}} - T^a\right) + T^a \tag{33}$$

where T_k^{end} and T_k^{start} are the temperatures at the end and the start of the pipe in °C, T^a is the ambient temperature in °C, λ_k is a heat transfer coefficient of the pipe, and C_p is the specific heat of water.

In network 1, node 0^c represents a GG, node 1^c a GB, and node 2^c a CHP. We use linear models for the GB and CHP, and use the same nonlinear model as proposed in [10] for the GG:

$$\begin{aligned} f_0^c(q_0^c, P_0^c) &= \text{GHV}q_0^c - a(P_0^c)^2 + bP_0^c \\ &\quad + c + \left|d\sin(e(P^{\min} - P_0^c))\right| = 0 \\ f_1^c(q_1^c, \varphi_1^c) &= \varphi_1^c - \eta_{\text{GB}}\text{GHV}q_1^c = 0 \\ f_2^c(q_2^c, P_2^c, \varphi_2^c) &= \text{GHV}q_2^c - \frac{P_2^c}{\eta_{\text{CHP}}} - \frac{\varphi_2^c}{\eta_{\text{CHP}}} = 0 \end{aligned} \tag{34}$$

with GHV the GHV of gas, a, b, c, d, and e parameters of the GG, $P^{\min}$ the minimum power produced by the GG, and η_{GB} and η_{CHP} the efficiencies of the GB and the CHP.

In network 2, both nodes represent an EH. The coupling matrices are chosen such that the EHs model the same conversion of energy as the coupling components in network 1:

$$\begin{aligned} f_0^c(q_0^c, P_0^c, \varphi_0^c) &= \begin{pmatrix} P_0^c \\ \varphi_0^c \end{pmatrix} - \begin{pmatrix} \nu_0\eta_{\text{GG}} \\ (1-\nu_0)\eta_{\text{GB}} \end{pmatrix}(\text{GHV}q_0^c) \\ f_1^c(q_1^c, P_1^c, \varphi_1^c) &= \begin{pmatrix} P_1^c \\ \varphi_1^c \end{pmatrix} - \begin{pmatrix} \nu_1\eta_{\text{CHP}} \\ (1-\nu_1)\eta_{\text{CHP}} \end{pmatrix}(\text{GHV}q_1^c) \end{aligned} \tag{35}$$

with ν_0 and ν_1 dispatch factors, and η_{GG} the efficiency of the (linearized) GG. To ensure consistency with network 1, we take

$$\begin{aligned} \eta_{\text{GG}} &= \frac{\tilde{P}_0^c}{\text{GHV}\tilde{q}_0^c} \approx 0.45 \\ \nu_0 &= \frac{\tilde{q}_0^c}{\tilde{q}_0^c + \tilde{q}_1^c} \approx 0.77 \\ \nu_1 &= \frac{\tilde{P}_2^c}{\tilde{P}_2^c + \tilde{\varphi}_2^c} \approx 0.27 \end{aligned} \tag{36}$$

with $\tilde{q}^c$, $\tilde{P}^c$, and $\tilde{\varphi}^c$ the coupling energies of network 1.

Table 4
Parameters of the links and other elements in both example networks, per carrier.

Carrier	Link parameters				Other parameters								
Gas	L [m]	D [m]	ϵ [m]	r	T_n [K]	T [K]	R_{air} [J/(kg K)]	p_n [Pa]	Z	S	μ [m^2/s]	GHV [j/kg]
	30×10^3	0.15	0.05×10^{-3}	1.3	273.15	281.15	287.008	1.01325×10^5	0.8	0.6106	0.288×10^{-6}	5.4297×10^7
Electricity	b [S]	g [S]										
	-5.941	0.5941										
Heat	L [m]	D [m]	ϵ [m]	λ [W/(m K)]	ρ [kg/m^3]	μ [m^2/s]	C_p [J/(kg K)]	T^a [°C]				
	30×10^3	0.15	1.25×10^{-3}	0.2	960	0.294×10^{-6}	4.182×10^3	10				
	Unit parameters											
Coupling	a	b	c	d	e	p^{min}	η_{GB}	η_{CHP}	η_{GG}	γ_0	γ_1	
	2.931×10^{-9}	1.1724	4.3965×10^7	4.3965×10^6	5×10^{-7}	0	0.88	0.88	0.45	0.77	0.27	

5.2. Node types

In [5] and [10], the coupling heat powers are assumed known. We assume all coupling energies unknown, but assume T^o of all coupling nodes known. As BCs for the heat terminal links, $T^o_{i,l}$ is specified instead of $\Delta T_{i,l}$. For network 1, the coupling models require 5 additional BCs if T^o is known for all coupling nodes. In comparison, the coupling models for network 2 only require 3 additional This shows that the coupling units determine the additional BCs required. Conversely, requiring realistic or physical BCs for all nodes limits the coupling units that can be used to couple SCNs. Table 5 gives the nodes types used for both networks. These node sets are not unique, for instance, instead of the node set given for network 2, node 2^h can be taken as sink reference node and T^o for node 1^c can be kept as unknown. The corresponding system of load flow equations would then also be solvable for suitable initial conditions.

With these node sets, the system of load flow equations for the MES (18) consists of 32 equations and variables for network 1, and 33 equations and variables for network 2. To solve the systems of equations, we use scaled NR (24) with a tolerance of 10^{-6}. As base values we take $q_b = 1$ kg/s, $p^g_b = 1 \times 10^5$ Pa, $|V|_b = 10/\sqrt{3} \times 10^3$ V, $m_b = 1$ kg/s, $p^h_b = 1 \times 10^5$ Pa, $T_b = 130$ °C, $|S|_b = 10 \times 10^6$ W, $\varphi_b = 10 \times 10^6$ W, and $E^g_b = 10 \times 10^6$ W. We also solve the load flow problem using per unit scaling, with the same base values, and unscaled NR (21) with a tolerance of 10^{-6}.

The values used for the BCs are given in Tables 8–14, and the initial guess to the solution vector for both matrix scaling and per unit scaling is given in Table 6. In the heat network, the values for the head $h = \frac{p^h}{\rho g}$, with g the gravitational constant, are given instead of the nodal pressure. The nodal pressure is still used in the calculations. Table 7 and Fig. 5 give the error of the scaled system of equations using matrix scaling and per unit scaling for every iteration of NR. This shows that scaling by matrix multiplication is indeed equivalent to scaling using the per unit system, when the same base values are used, and the parameters in the load flow equations are scaled accordingly for the per unit system.

Tables 8–14 give the results for both network 1 and 2. For comparison, the results found in [5,10] are also listed. Our results for network 1 match the ones found in [10], except for the gas network. However, plugging in their pressures values in the flow Eq. (25) does not give their gas pipe flows. The ratio between their presented gas flows and the flows obtained from the flow equations seems to be a factor ln10.

Our results for network 2 match the ones found in [5], except for small differences in the heat network. In [5], a different model for sinks and sources is used. That is, they use $\Delta T_{i,l} = T^s_i - T^r_i$ for both sinks and sources, whereas we use the temperature difference in (11). Second, they use a different thermal model for the pipe lines.

The other small differences are due to differences in BCs, and different formulations of the system of load flow equations. In [5,10], the heat powers of the coupling components are assumed known, while, for our BCs, the heat network determines the required heat power. Through the coupling equations, the coupling gas flows and active power can be determined, which are then effectively a specified value from the perspective of the single-carrier gas and electrical networks. Due to small differences in the coupling heat powers between our result and the one presented in [5,10], the result in the gas and electrical part is also slightly different.

6. Conclusion

We developed a graph-based model framework for steady-state load flow analysis of general multi-carrier energy systems (MESs), consisting of gas, electricity, and heat. The framework is based on connecting the single-carrier networks (SCNs) to a heterogeneous coupling node, using

Table 5
Node type sets used for the example networks.

Network 1				Network 2			
Node	Node type	Specified	Unknown	Node	Node type	Specified	Unknown
0^g	Ref.	p^g	q	0^g	Ref.	p^g	q
1^g	Load	q	p^g	1^g	load	q	p^g
2^g	Ref. load	p^g, q	-	2^g	load	q	p^g
3^g	Load	$q = 0$	p^g	3^g	load	$q = 0$	p^g
0^e	PQVδ	P, Q, $\|V\|$, δ	–	0^e	PQVδ	P, Q, $\|V\|$, δ	-
1^e	Load	P, Q	$\|V\|$, δ	1^e	load	P, Q	$\|V\|$, δ
2^e	PQV	P, Q, $\|V\|$	δ	2^e	PQV	P, Q, $\|V\|$	δ
0^h	Ref.	p^h, $m = 0$	T^r, T^s	0^h	Ref.	p^h, $m = 0$	T^r, T^s
1^h	Sink	T^o and $\varphi > 0$	T^r, T^s, p^h, m	1^h	sink	T^o and $\varphi > 0$	T^r, T^s, p^h, m
2^h	Sink Ref.	T^o, $\varphi > 0$, p^h	T^r, T^s, m	2^h	sink	T^o and $\varphi > 0$	T^r, T^s, p^h, m
0^c	Standard	–	–	0^c	temp.	T^o	–
1^c	Temp.	T^o	–	1^c	temp.	T^o	–
2^c	Temp.	T^o	–				

Table 6
Initial values of x^0 used for NR, for the example networks.

Node	Network 1 Initial value	Network 2 Initial value
0^g	–	–
1^g	$p^g = 40 \times 10^5$ Pa	$p^g = 45 \times 10^5$ Pa
2^g	–	$p^g = 47 \times 10^5$ Pa
3^g	$p^g = 40 \times 10^5$ Pa	$p^g = 45 \times 10^5$ Pa
0^e	–	–
1^e	$\|V\| = 10/\sqrt{3} \times 10^3$ V, $\delta = 0$ rad	$\|V\| = 10/\sqrt{3} \times 10^3$ V, $\delta = 0$ rad
2^e	$\delta = 0$ rad	$\delta = 0$ rad
0^h	$T^r = 50$ °C, $T^s = 100$ °C	$T^r = 50$ °C, $T^s = 100$ °C
1^h	$T^r = 50$ °C, $T^s = 120$ °C, $h =$ 10 m, $m = 20$ kg/s	$T^r = 50$ °C, $T^s = 120$ °C, $h =$ 254.3706 m, $m = 20$ kg/s
2^h	$T^r = 50$ °C, $T^s = 120$ °C, $m =$ 20 kg/s	T^r, $= 50$ °C, $T^s = 120$ °C, $h =$ 4300 m, $m = 20$ kg/s
0^c	$q = 2.19223$ kg/s, $P =$ 50×10^6 W, $Q = 0$ W	$q = 2.19223$ kg/s, $P =$ 50×10^6 W, $Q = 0$ W, $m = 10$ kg/ s, $\varphi = 30 \times 10^6$ W
1^c	$q = 0.65767$ kg/s, $m = 10$ kg/s, φ $= 30 \times 10^6$ W	$q = 0.65767$ kg/s, $P =$ 10×10^6 W, $Q = 0$ W, $m = 10$ kg/ s, $\varphi = 25 \times 10^6$ W
2^c	$q = 0.65767$ kg/s, $P =$ 10×10^6 W, $Q = 0$ W, $m = 10$ kg/ s, $\varphi = 25 \times 10^6$ W	

homogeneous dummy links, to form one multi-carrier network. The load flow equations for the SCNs and for the coupling nodes are collected into one integrated system of nonlinear load flow equations. The framework allows for a variety of single-carrier components and load flow models. The coupling node allows for bidirectional flow, and can represent a variety of couplings, such as a single converter component, an energy hub, or a complete heterogeneous network. Having the coupling node represent a complete heterogeneous network could lead to a hierarchical approach.

We assume the coupling energies unknown, since the SCNs would effectively be decoupled otherwise. This requires additional boundary conditions in the single-carrier part of the network, leading to new node types. Using these new node types, the system of nonlinear load flow equations is formulated. Due to the introduction of the heterogeneous coupling node, the SCNs are independent of each other. The interdependencies enter the system of equations through the coupling part. This approach leads to a Jacobian matrix with a distinct structure, in which the submatrices are not necessarily square. However, the node types and location of the coupling nodes in the graph must be carefully chosen. Certain combinations of node types, or graph topologies, can result in systems of equations that are not (uniquely) solvable. This is still an open problem. Our systematic approach to the graph representation of MESs, and corresponding formulation of the system of load flow equations, provides insight into which coupling nodes and node types lead to such unsolvable systems.

Using our proposed model framework, we modeled one MES consisting of gas, electricity, and heat. Two multi-carrier networks were used to model this MES. They have the same SCNs, but use different coupling components. This example shows that our proposed model framework can be used to model steady-state load flow for general

Table 7
Error of NR per iteration for network 1 and network 2, using matrix scaling and per unit scaling. The error is $||D_F F_a(x^k)||_2$ for matrix scaling, and $||F_{\text{p.u.}}(x^k)||_2$ for per unit scaling.

iter.	Network 1			Network 2		
	$\|\|D_F F_a(x^k)\|\|_2$	$\|\|F_{\text{p.u.}}(x^k)\|\|_2$	$\frac{\|\|\, \|\|D_F F_a(x^k)\|\|_2 - \|\|F_{\text{p.u.}}(x^k)\|\|_2 \,\|}{\|\|D_F F_a(x^k)\|\|_2}$	$\|\|D_F F_a(x^k)\|\|_2$	$\|\|F_{\text{p.u.}}(x^k)\|\|_2$	$\frac{\|\|\, \|\|D_F F_a(x^k)\|\|_2 - \|\|F_{\text{p.u.}}(x^k)\|\|_2 \,\|}{\|\|D_F F_a(x^k)\|\|_2}$
0	2.1756×10^3	2.1756×10^3	2.0903×10^{-16}	3.1521×10^3	3.1521×10^3	4.3280×10^{-16}
1	9.2049×10^2	9.2049×10^2	4.9403×10^{-16}	6.8240×10^2	6.8240×10^2	3.3320×10^{-16}
2	1.6054×10^2	1.6054×10^2	5.3111×10^{-16}	5.3596×10^1	5.3596×10^1	3.1818×10^{15}
3	2.4988×10^{-1}	2.4988×10^{-1}	1.5817×10^{-13}	5.4506×10^{-1}	5.4506×10^{-1}	5.6319×10^{-13}
4	5.9439×10^{-4}	5.9439×10^{-4}	3.0217×10^{-10}	5.0576×10^{-5}	5.0576×10^{-5}	6.8517×10^{-9}
5	5.9071×10^{-7}	5.9071×10^{-7}	2.0139×10^{-7}	1.6610×10^{-8}	1.6610×10^{-8}	7.4091×10^{-6}

Table 8
Results for the gas network, for network 1 (a), from [10] (b), for network 2 (c), and from [5] (d).

	p [bar]				q^{inj} [10^3 m^3/h]					q [10^3 m^3/h]			
Node	(a)	(b)	(c)	(d)	(a)	(b)	(c)	(d)	Link	(a)	(b)	(c)	(d)
0	50.000	50.000	50.000	–	−46.715	−47.108	−46.715	–	0–1	18.233	29.831	18.233	–
1	29.102	40.816	29.102	–	10.865	10.000	10.865	–	0–2	16.408	4.810	16.408	–
2	34.077	49.783	34.077	–	20.000	20.000	20.000	–	3–2	7.368	18.966	7.368	–
3	37.833	53.061	37.833	–	0.000	–	0.000	–	1–3	7.368	18.966	7.368	–

Table 9
Results for the electrical network, for network 1 (a) and from [10] (b).

	$\lvert V\rvert$ [p.u.]		δ [°]		S^{inj} [MW]	
Node	(a)	(b)	(a)	(b)	(a)	(b)
0	1.060	1.060	0.000	0.000	0.145 + 0.000ι	0.145 + 0.000ι
1	0.980	0.980	−6.989	−7.022	30.000 + 15.000ι	30.000 + 15.000ι
2	1.000	1.000	−6.048	−6.116	30.136 + 15.000ι	30.136 + 15.000ι
	S_{ij} [MW]		S_{ji} [MW]		S_{ij}^{loss} [MW]	
Link	(a)	(b)	(a)	(b)	(a)	(b)
0–1	26.862 + 15.801ι	26.981 + 15.811ι	−26.429 −11.479ι	−26.545 −11.459ι	0.432 + 4.322ι	0.435 + 4.352ι
0–2	23.492 + 11.551ι	23.741 + 11.552ι	−23.187 −8.501ι	−23.430 −8.450ι	0.305 + 3.050ι	0.310 + 3.102ι
1–2	−3.571 −3.521ι	−3.455 −3.541ι	3.584 + 3.652ι	3.467 + 3.669ι	0.013 + 0.131ι	0.013 + 0.127ι
Total					0.750 + 7.502ι	0.758 + 7.581ι

Table 10
Results for the electrical network, for network 2 (c) and from [5] (d).

	$\lvert V\rvert$ [p.u.]		δ [°]		S^{inj} [MW]	
Node	(c)	(d)	(c)	(d)	(c)	(d)
0	1.060	1.060	0.000	0.000	0.145 + 0.000ι	0.145 + 0.000ι
1	0.980	0.980	−6.989	−7.022	30.000 + 15.000ι	30.000 + 15.000ι
2	1.000	1.000	−6.048	−6.116	30.136 + 15.000ι	30.136 + 15.000ι
	S_{ij} [MW]		S_{ji} [MW]		S_{ij}^{loss} [MW]	
Link	(c)	(d)	(c)	(d)	(c)	(d)
0–1	26.861 + 15.801ι	26.981 + 15.811ι	−26.429 −11.479ι	–	0.432 + 4.322ι	0.435 + 4.352ι
0–2	23.492 + 11.551ι	23.740 + 11.552ι	−23.187 −8.501ι	–	0.305 + 3.049ι	0.310 + 3.102ι
1–2	−3.571 −3.521ι	−3.455 −3.541ι	3.584 + 3.652ι	–	0.013 + 0.131ι	0.013 + 0.127ι
Total					0.750 + 7.502ι	0.758 + 7.581ι

Table 11
Results for the hydraulic part of the heat network, for network 1 (a), from [10] (b), for network 2 (c), and from [5] (d).

	h [m]				m^{inj} [kg/s]					m [kg/s]			
Node	(a)	(b)	(c)	(d)	(a)	(b)	(c)	(d)	Link	(a)	(b)	(c)	(d)
0	5517.000	–	5517.000	5517.000	0.000	–	0.000	–	0–1	64.687	64.694	64.687	65.962
1	225.103	–	225.066	10.666	121.223	–	121.223	–	0–2	31.408	31.453	31.409	29.893
2	4268.109	–	4268.046	4383.800	65.026	–	65.026	–	1–2	−56.537	−56.533	−56.537	−58.778

MESs. Moreover, our framework can be used with different components and models, both in the SCNs and for the coupling units. Therefore, our framework includes and extends the currently available load flow models for MESs.

Future work includes optimal load flow models for general MES, and application of the proposed framework to large MESs.

CRediT authorship contribution statement

A.S. Markensteijn: Conceptualization, Methodology, Software, Writing - original draft. **J.E. Romate:** Conceptualization, Funding acquisition, Methodology, Project administration, Writing - review & editing. **C. Vuik:** Supervision, Writing - review & editing.

Table 12
Results for the thermal part of the heat network, for network 1 (a), from [10] (b), for network 2 (c), and from [5] (d).

	T^s [°C]				T^r [°C]				φ^{inj} [MW]					φ^{loss} [MW]			
Node	(a)	(b)	(c)	(d)	(a)	(b)	(c)	(d)	(a)	(b)	(c)	(d)	Link	(a)	(b)	(c)	(d)
0	120.000	120.000	120.000	120.000	48.680	48.681	48.680	48.536	0.000	0.000	0.000	0.000	0–1	0.890	0.890	0.890	0.890
1	119.040	119.037	119.039	117.090	50.000	50.000	50.000	50.000	35.000	35.000	35.000	35.000	0–2	0.877	0.877	0.877	0.873
2	123.546	123.541	123.546	123.541	49.534	49.534	49.534	49.035	20.000	20.000	20.000	20.000	1–2	0.910	0.910	0.910	0.884
Total														2.677	2.677	2.677	2.647

Table 13
Results for the coupling part of the network, for network 1 (a) and from [10] (b).

	q [10^3 m^3/h]		P [MW]		Q [MVAr]		m^{inj} [kg/s]		φ [MW]		T^o [°C]	
Unit	(a)	(b)	(a)	(b)	(a)	(b)	(a)	(b)	(a)	(b)	(a)	(b)
GG	9.338	9.450	50.499	50.866	27.352	27.363	–	–	–	–	–	–
GB	2.736	3.018	–	–	–	–	96.095	–	28.661	28.677	120.000	–
CHP	3.776	3.776	10.533	10.173	10.151	10.218	90.154	–	29.016	29.000	126.493	–

Table 14
Results for the coupling part of the network, for network 2 (c) and from [5] (d).

	q [10^3 m^3/h]		P [MW]		Q [MVAr]		m^{inj} [kg/s]		φ [MW]		T^o [°C]	
Unit	(c)	(d)	(c)	(d)	(c)	(d)	(c)	(d)	(c)	(d)	(c)	(d)
EH 0	12.074	–	50.498	50.866	27.352	27.363	96.096	–	28.662	28.647	120.000	–
EH 1	3.776	–	10.533	10.173	10.151	10.218	90.153	–	29.015	29.000	126.493	–

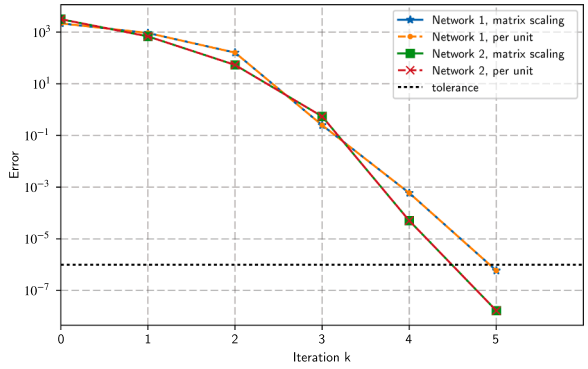

Fig. 5. Convergence of NR for network 1 and network 2, using matrix scaling and per unit scaling. The error is $||D_F F_a(x^k)||_2$ for matrix scaling, and $||F_{\text{p.u.}}(x^k)||_2$ for per unit scaling.

Declaration of Competing Interest

The authors declare that they have no known competing financial interests or personal relationships that could have appeared to influence the work reported in this paper.

References

[1] Mancarella P. MES (multi-energy systems): an overview of concepts and evaluation models. Energy 2014;65:1–17. https://doi.org/10.1016/j.energy.2013.10.041.
[2] Geidl M, Andersson G. Optimal power flow of multiple energy carriers. IEEE Trans Power Syst 2007;22:145–55. https://doi.org/10.1109/TPWRS.2006.888988.
[3] Wasilewski J. Integrated modeling of microgrid for steady-state analysis using modified concept of multi-carrier energy hub. Int J Electrical Power Energy Syst 2015;73:891–8. https://doi.org/10.1016/j. ijepes.2015.06.022.
[4] Long S, Parisio A, Marjanovic O. A conversion model for nodes in multi-energy systems. 2017 IEEE Manchester PowerTech Powertech; 2017. https://doi.org/10.1109/PTC.2017.7981052.
[5] Ayele GT, Haurant P, Laumert B, Lacarrière B. An extended energy hub approach for load flow analysis of highly coupled district energy networks: illustration with electricity and heating. Appl Energy 2018;212:850–67. https://doi.org/10.1016/j.apenergy.2017.12.090.
[6] An S, Li Q, Gedra T. Natural gas and electricity optimal power flow. In: IEEE PES transmission and distribution conference and exposition; 2003. p. 138–43. doi:10.1109/TDC.2003.1335171, arXiv:1011.1669v3.
[7] Martinez-Mares A, Fuerte-Esquivel CR. A Unified gas and power flow analysis in natural gas and electricity coupled networks. IEEE Trans Power Syst 2012;27:2156–66. https://doi.org/10.1109/TPWRS.2012.2191984.
[8] Pan Z, Guo Q, Sun H. Interactions of district electricity and heating systems considering time-scale characteristics based on quasi-steady multi-energy flow. Appl Energy 2016;167:230–43. https://doi.org/10.1016/j.apenergy.2015.10.095.
[9] Liu X, Jenkins N, Wu J, Bagdanavicius A. Combined analysis of electricity and heat networks. Appl Energy 2016;162:1238–50. https://doi.org/10.1016/j.egypro.2014.11.928.
[10] Shabanpour-Haghighi A, Seifi AR. An integrated steady-state operation assessment of electrical, natural gas, and district heating networks. IEEE Trans Power Syst 2016:3636–47. https://doi.org/10.1109/TPWRS.2015.2486819.
[11] Abeysekera M, Wu J. Method for simultaneous power flow analysis in coupled multi-vector energy networks. Energy Procedia 2015;75:1165–71. https://doi.org/10.1016/j.egypro.2015.07. 551.
[12] Liu X, Mancarella P. Modelling, assessment and Sankey diagrams of integrated electricity-heat-gas networks in multi-vector district energy systems. Appl Energy 2016;167:336–52. https://doi.org/10.1016/j.apenergy.2015.08.089.
[13] Frederiksen S, Werner S. District heating and cooling. Studentlitteratur AB; 2014.
[14] Kuosa M, Kontu K, Mäkilä T, Lampinen M, Lahdelma R. Static study of traditional and ring networks and the use of mass flow control in district heating applications. Appl Therm Eng 2013;54:450–9. https://doi.org/10.1016/j.applthermaleng.2013.02.018.
[15] Osiadacz AJ. Simulation and analysis of gas networks. London: Spon; 1987.
[16] Schavemaker P, Van der Sluis L. Electrical power system essentials. Chichester, West Sussex: Wiley; 2008.
[17] Stott B. Review of load-flow calculation methods. Proc IEEE 1974;62:916–29. https://doi.org/10.1109/PROC.1974.9544.
[18] Sereeter B, Vuik C, Witteveen C. On a comparison of Newton-Raphson solvers for

power flow problems. J Comput Appl Math 2019;360:157–69. https://doi.org/10.1016/j.cam.2019.04.007.
[19] Arsene CTC, Bargiela A, Al-Dabass D. Modelling and simulation of water systems based on loop equations. J Simul 1989;5:1–2.
[20] Liu X, Jenkins N, Wu J. Optimal coordinated operation of a multi-energy community considering interactions between energy storage and conversion devices. Appl Energy 2019;248:256–73.
[21] Dennis JE, Schnabel RB. Numerical methods for unconstrained optimization and nonlinear equations. Prentice Hall, Inc; 1983.
[22] Markensteijn AS, Romate JE, Vuik C. On the solvability of steady-state load flow problems for multi-carrier energy systems. IEEE Milan PowerTech; 2019. p. 2019.
[23] Duquette J, Rowe A, Wild P. Thermal performance of a steady state physical pipe model for simulating district heating grids with variable flow. Appl Energy 2016;178:383–93.